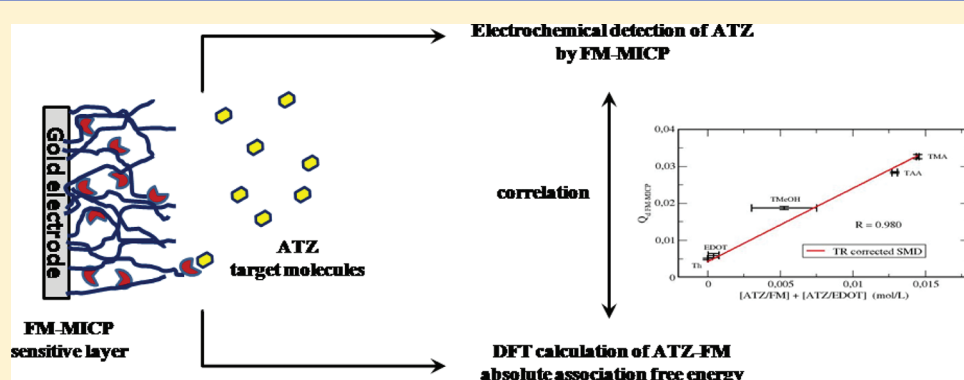


Influence of the Chemical Functionalities of a Molecularly Imprinted Conducting Polymer on Its Sensing Properties: Electrochemical Measurements and Semiempirical DFT Calculations

Youssef Lattach,[†] Pierre Archirel,^{*,†,‡} and Samy Remita^{*,†,‡}

[†]Laboratoire de Conception de Capteurs Chimiques et Biologiques, LC3B, Conservatoire National des Arts et Métiers, CNAM, 292 rue Saint-Martin, 75141 Paris Cedex 03, France

[‡]Laboratoire de Chimie Physique, LCP, UMR 8000 CNRS, Université Paris-Sud 11, Bât. 349, Campus d'Orsay, 15 Avenue Jean Perrin, 91405 Orsay Cedex, France



ABSTRACT: Starting from thiophene-based functional monomers (FM), namely, TMA, TAA, TMMeOH, EDOT, and Th, bonded to atrazine (ATZ) target molecules into FM/ATZ prepolymerization dimers in acetonitrile solutions, differently functionalized molecularly imprinted conducting polymers (FM-MICP) are electrosynthesized and then washed and used as sensitive layers for ATZ recognition. Sensitivity of these layers toward ATZ, which is quantified by cyclic voltammetric measurements, decreases in the following order of functional monomers: TMA, TAA, TMMeOH, EDOT, and Th. Absolute values of the FM-ATZ dimerization free energies are calculated with the help of DFT/PCM calculations and of an empirical correction of the entropy effects, using a modified Wertz formula. A strong correlation is found between FM-MICP sensitivity and the amount of FM/ATZ prepolymerization complexes.

1. INTRODUCTION

Molecularly imprinted polymers (MIP), which are synthesized through polymerization in the presence of a template target molecule, have now established themselves as materials able to recognize with high selectivity a given target or even a class of target molecules.^{1–4} Indeed, starting from well-functionalized monomers, MIP synthesis leads to the formation into the polymeric matrix of specific cavities which demonstrate very interesting recognition properties toward the target after its removal. In this approach, the template can be linked to the functional monomers, extracted, and consequently recognized by the functionalized polymeric binding sites through noncovalent bonds (mostly hydrogen bonds)^{1,2} or through reversible covalent bonds.^{3,4} Nevertheless, the most widely applied method to generate molecularly binding sites is based on noncovalent interactions implying the self-assembly, prior to polymerization, of the template molecule with functional monomers (in the presence of linkers or cross-linking monomers). Thus, the goal of several experimental as well as theoretical works was the study and the optimization of these monomer/target prepolymerization complexes^{5–7} with the aim

to optimize MIP performance through the selection of suitable functional monomers.⁸

Conducting materials, such as conducting polymers (CP), appear very well designed for their use as sensitive layers in a recognition matrix, allowing direct and real time transduction of the recognition event into an electronic signal. Conducting polymers, which present π -conjugated structures, are characterized by a high electrical conductivity and a good electrochemical reversibility, which justify their use as transducers in the fabrication of electrochemical sensors dedicated to the detection of small molecules.^{9–12} The use of conducting polymers as substrates, which can be chemically functionalized with the required “probes”, leads to highly integrated sensing systems, bearing at the same time the recognition moieties and the required transducing properties of the sensor. The synthesis of functionalized CP in the presence of a target molecule leads to interesting materials, namely, molecularly imprinted conducting

Received: July 27, 2011

Revised: December 14, 2011

Published: December 29, 2011

polymers (MICP), which we described in our previous work¹² and which we integrated as sensitive layers in electrochemical sensors.^{13,14} These materials present high recognition specificity together with high sensitivity, since they combine the properties of molecularly imprinted polymers (MIP) and those of conducting polymers (CP). As a consequence, the design and the development of such materials in the field of sensors seem to be a promising way for the selective and real time recognition of small target molecules.

The detection of small organic molecules remains an open challenge, since their interaction with pendent binding sites present in the MIP or the MICP polymer matrix is not really understood. In addition, the factors which contribute to the binding, such as ionization state, polarity, and hydrophobicity, need to be identified and quantified. An ideal sensor must be able to specifically detect very small amounts of a target. This implies, in our case, the development of the more specific and the more sensitive MICP layer. In particular, this means that the functionalized probes present in the polymer matrix must be spatially well distributed and must present a very high specific affinity toward the target in a given medium (polar or apolar). The choice of the chemical functionalities of the monomers, as polymer starting blocks, appears then determining. These functionalities are first involved during the association of the monomers with the targets in the prepolymerization complexes. They are second implied during the binding of the targets with the polymer matrixes. A strong interaction of the probes with the targets must then lead to a MICP matrix with highly specific imprints and, as a consequence, to a very sensitive functionalized layer.

In the present paper, we experimentally and theoretically study the influence of the nature of the chemical functionalities of a polythiophene-based MICP on its ability to bind and then to detect a target molecule, namely, atrazine. Differently functionalized thiophene-based monomers are used in order to form prepolymerization complexes with atrazine in acetonitrile solvent. The polymerization of the thiophene-based monomers in the presence of atrazine leads to differently functionalized MICP. The recognition of additional amounts of atrazine is quantified by electrochemical measurements (section 2). The binding free energies of the different prepolymerization dimers involved are calculated using a quantum chemical approach (section 3). We find a strong correlation between the concentrations of the prepolymerization complexes deduced from the binding energies and the sensitivity of the MICP-based sensor (section 4).

2. ELECTROCHEMICAL EVALUATION OF THE SENSING PROPERTIES

2.1. Materials. Pesticide used as a target molecule, namely, atrazine (2-chloro-4-(ethylamino)-6-(isopropylamino)-1,3,5-triazine), ATZ, was obtained from Sigma (Figure 1). The 3,4-ethylenedioxothiophene, EDOT, purchased from AKSCI, was used as a linker and/or as a functional monomer (FM) and was distilled under reduced pressure before use (Figure 1). 3-Thiopheneacetic acid, TAA, provided from Acros, 3-thiophenemalonic acid, TMA, 3-thiophenemethanol, TMeOH, and thiophene, Th, were purchased from Aldrich and used as functional monomers (FM) without further purification (Figure 1). Lithium perchlorate, LiClO₄, purchased from Aldrich, was utilized as a supporting electrolyte. All of these chemicals were dissolved in acetonitrile solvent, ACN, obtained from Acros Chemicals. ACN was distilled prior to use and purged with argon for 30 min.

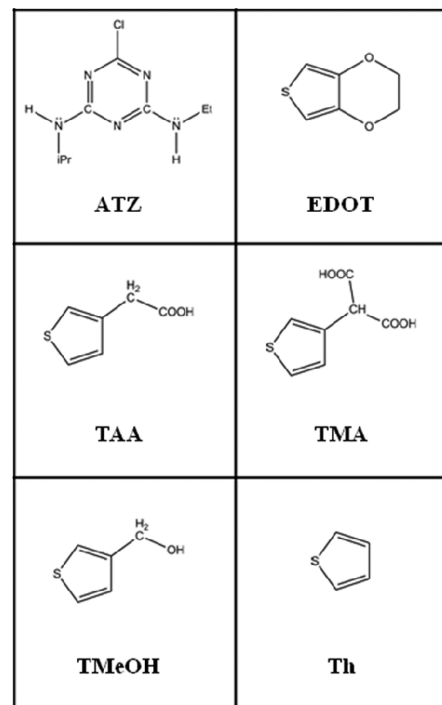


Figure 1. Chemical structures of the target molecule (ATZ) and of the different FM functional monomers (EDOT, TAA, TMA, TMeOH, and Th). EDOT is also, in all the cases, the linker. For the ATZ molecule, the *trans*-isopropyl, *cis*-ethyl conformer is represented.

Methanol, MeOH, and acetic acid, CH₃COOH, used as extraction solvents were purchased from VWR and Acros, respectively.

2.2. Electrochemical Polymerization and Electrochemical Measurements. In this work, molecularly imprinted conducting polymers or copolymers, MICP-based sensitive layers, were electrochemically obtained by polymerization of EDOT monomers in the presence of ATZ target molecules (FM = EDOT) or by copolymerization of EDOT with another kind of functional monomers (FM = TAA, TMA, TMeOH, or Th) associated by noncovalent interactions with ATZ target molecules (Figure 2A, electrosynthesis). For clarity, for all functional monomers (FM) used, the obtained poly(EDOT/ATZ) polymers and poly(EDOT-co-FM/ATZ) copolymers are noted FM-MICP.

For FM-MICP preparation, FM functional monomers (EDOT, TAA, TMA, TMeOH, or Th) at a concentration of 3×10^{-2} mol L⁻¹ were dissolved in acetonitrile solvent, in the presence of LiClO₄ (0.1 mol L⁻¹, as supporting electrolyte), together with ATZ molecules at a concentration of 1.5×10^{-2} mol L⁻¹. A sufficient lap time of 10 min was used in order to favor the association between FM and ATZ, through noncovalent interactions, in FM/ATZ prepolymerization complexes. Then, EDOT, at a concentration of 7.5×10^{-3} mol L⁻¹, was added as a linker, before electropolymerization, to each FM/ATZ solution.

Another type of films, nonimprinted conducting polymers or copolymers, NICP, was also electrochemically prepared but in the absence of target molecules in the prepolymerization media (Figure 2B, electrosynthesis). NICP polymers were synthesized by polymerization of EDOT monomers (FM = EDOT), while NICP copolymers were obtained from the copolymerization of EDOT monomers with another kind of functional monomers

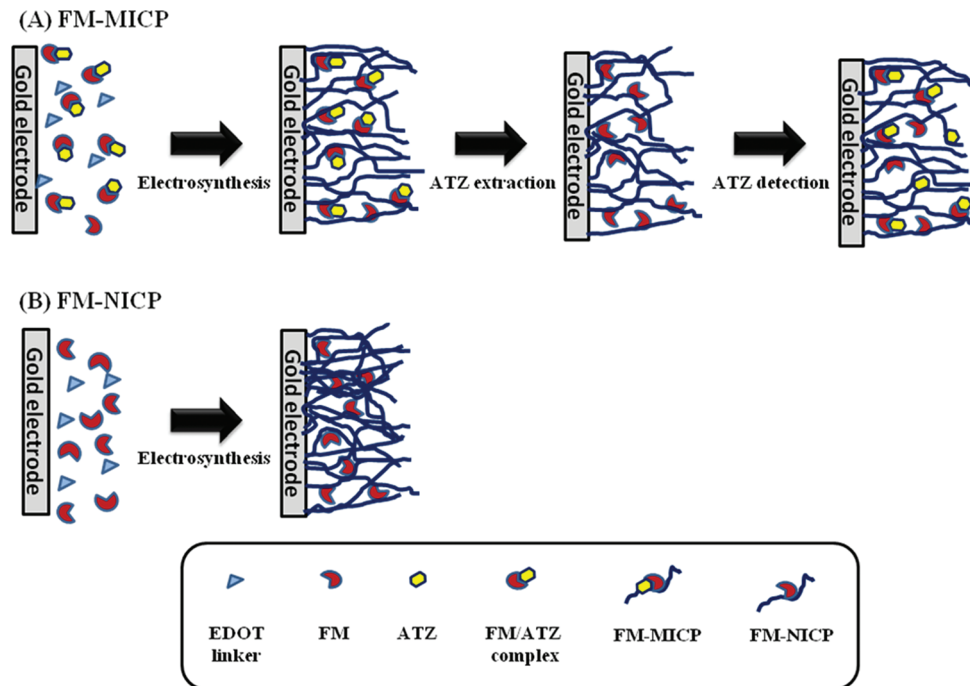


Figure 2. (A) Electrosynthesis and use for ATZ detection of FM-MICP. (B) Electrosynthesis of FM-NICP. The FM functional monomers are TMA, TAA, TMeOH, EDOT, or Th.

(FM = TAA, TMA, TMeOH, or Th). For clarity, in the case of all functional monomers (FM) used, the obtained poly(EDOT) polymers and poly(EDOT-*co*-FM) copolymers are noted FM-NICP.

For FM-NICP preparation, FM functional monomers (EDOT, TAA, TMA, TMeOH, or Th) at a concentration of 3×10^{-2} mol L⁻¹ were dissolved in acetonitrile solvent, in the presence of LiClO₄ (0.1 mol L⁻¹, as supporting electrolyte) but in the absence of ATZ molecules. Then, EDOT, at a concentration of 7.5×10^{-3} mol L⁻¹, was added as a linker to each FM solution, before electropolymerization.

Electropolymerizations were carried out in a conventional three-electrode electrochemical cell. The working electrodes were gold surfaces with a surface area of 3.14 mm² (from Bioanalytical Systems), rinsed with distilled water and ethanol, polished, and ultrasonically cleaned in distilled water. These electrodes were finally rinsed with ACN solvent and immersed in the prepolymerization solutions before being used as substrates for the electropolymerization. Counter electrodes were stainless steel sheets, and all potentials were controlled vs Ag/AgNO₃ reference electrode for ACN (+0.29 vs SCE).¹⁵ Prior to all the experiments, the solutions were purged with argon. Such an inert atmosphere was maintained over all the solutions during the measurements.

In order to study the electrochemical behaviors of FM functional monomers as well as those of synthesized FM-MICP and FM-NICP films, cyclic voltammograms were recorded at a scan rate of 25 mV s⁻¹. All cyclic voltammograms were obtained by subtracting the background current corresponding to the electrolyte (0.1 mol L⁻¹ of LiClO₄ in ACN). Several preliminary experiments were performed in order to determine the oxidation potentials of the different FM functional monomers. Electrosynthesis of FM-MICP and FM-NICP films at the surface of gold electrodes, under potentiostatic conditions, was realized using a two-step chronoamperometry technique in the electrochemical cell. In the first step, the potential was switched

from 0.0 to 0.8 V for a period of ca. 10 s. Polymerization was achieved by a second step at a constant potential of 1.40 V vs Ag/AgNO₃. Specific times were used during this second chronoamperometric step in order to adjust the electro-polymerization charges at 3.14 mC for 3.14 mm² of the active surface of the working electrode (100 mC·cm⁻²). Cyclic voltammetric and amperometric measurements were performed on an EG&G model 263A potentiostat/galvanostat (Princeton Applied Research).

Contrarily to nonimprinted conducting FM-NICP films, molecularly imprinted FM-MICP layers were electrosynthesized in the presence of atrazine (Figure 2A, electrosynthesis). In order to remove the target molecules from FM-MICP matrices, by destroying the noncovalent intermolecular interactions which involve ATZ and polymerized functional monomers, a methanol/acetic acid solution (0.7:0.3 v/v) was used to wash the polymer-coated electrodes for 10 min.^{12–14,16} This washing step leads to the desired creation of molecular imprinted cavities within the copolymer matrixes of FM-MICP (Figure 2A, ATZ extraction). These cavities keep the memory of the interactions between FM functional monomers and ATZ molecules.^{12–14} Indeed, the spatial distribution of the polymerized functional monomers into the polymer matrixes allows the precise matching of additional ATZ molecules. Thus, the so-prepared washed FM-MICP modified electrodes can serve as electrochemical sensors to quantify the presence of new additional ATZ pesticides thanks to the establishment of new intermolecular FM/ATZ interactions between the probe-functionalized monomer units and the target molecules (Figure 2A, ATZ detection).

In order to check the ability of FM-MICP to interact with newly added pesticide targets (Figure 2A, ATZ detection), the modified gold electrodes were immersed for 10 min in ACN solutions containing ATZ at a concentration of 10^{-4} mol L⁻¹ in the presence of 0.1 mol L⁻¹ LiClO₄. The presence of added pesticide targets and consequently the recognition process was

then analyzed using an amperometric method. Modification of the electrochemical signatures of FM-MICP conducting polymers was monitored by the use of cyclic voltammetry. To quantify the current modifications when targets were added to the solution, the oxidation and reduction charges were calculated from cyclic voltammograms, by area integration under the curve of current versus time, this latter being related to the applied potential and to the scan rate.

2.3. FM-MICP and FM-NICP Electrosynthesis. In order to determine the “ideal” electropolymerization potential, which could be used whatever the functional monomer (FM) for FM-MICP and FM-NICP electrosynthesis, the redox behaviors of all functionalized monomers were studied using cyclic voltammetry. FM oxidation potentials, specified in Table 1,

Table 1. Oxidation Potentials of the Different FM Functional Monomers^a

	TMA	TAA	TMeOH	EDOT	Th
E_p (V vs Ag/AgNO ₃)	1.85	1.80	1.41	1.30	0.95

^aThese potentials were determined by cyclic voltammetry vs Ag/AgNO₃ at a sweep rate of 25 mV s⁻¹.

were determined vs Ag/AgNO₃ electrode at a scan rate of 25 mV s⁻¹.

In spite of the relative high oxidation potentials obtained for TMA and TAA in comparison with those of the other functional monomers, an electropolymerization potential of 1.40 V vs Ag/AgNO₃ was found to be sufficient to initiate EDOT polymerization as well as FM and EDOT copolymerization whatever the functional monomer. Applying such a

potential enabled in all the cases the synthesis of the different FM-MICP and FM-NICP films, respectively, in the presence and in the absence of ATZ (Figure 2A and B, electrosynthesis). In all cases, no polymer film overoxidation was observed. In addition, ATZ molecules did not show any electroactivity in the used potential range, as was already demonstrated in refs 12–14.

2.4. FM-MICP and FM-NICP Electrochemical Characterization. After the electrosynthesis step, the obtained FM-MICP and FM-NICP cyclic voltammograms were recorded for each FM functional monomer at the same scan rate of 25 mV s⁻¹. For illustration, Figure 3A displays voltammograms obtained in the case of TMA functional monomer, while Figure 3B displays those of Th.

The FM-MICP voltammograms are all different, as can be observed, for example, when comparing Figure 3A and B in the cases of TMA and Th as FM functional monomers. This indicates that the structure of the electrosynthesized FM-MICP films depends on the nature of the FM. This result demonstrates that in all the cases, in addition to EDOT, FM functional monomers are present in the polymer matrixes of FM-MICP. In our experimental conditions, the copolymerization is thus systematic. Since the FM-NICP voltammograms are also different from each other, one can deduce that FM functional monomers are also incorporated into the nonimprinted matrixes.

For each FM functional monomer, the FM-MICP voltammogram differs from the FM-NICP one, as can be observed in Figure 3A and B, respectively in the cases of TMA and Th. This is also the case for all the other FM functional monomers (TAA, TMeOH, and EDOT). Such a difference between

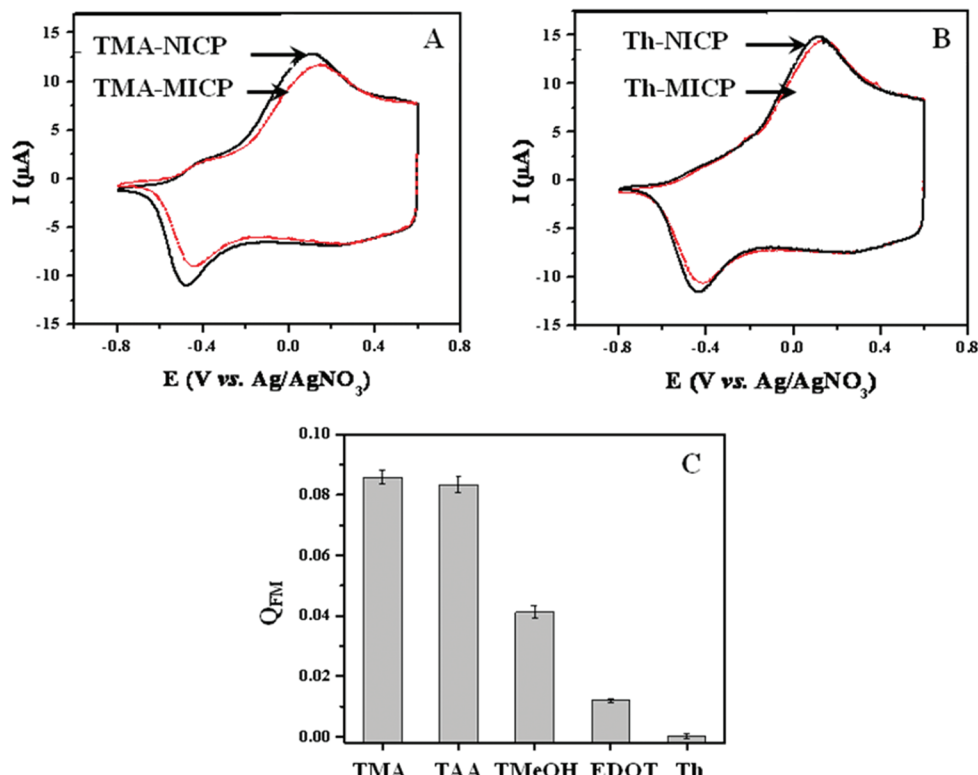


Figure 3. (A) Cyclic voltammograms of TMA-MICP and TMA-NICP films (FM = TMA). (B) Cyclic voltammograms of Th-MICP and Th-NICP films (FM = Th). All cyclic voltammograms were recorded in 0.1 M LiClO₄/ACN solutions at a scan rate of 25 mV s⁻¹. (C) Relative charges, Q_{FM} , measured for the different FM functional monomers (FM = TMA, TAA, TMeOH, EDOT, or Th). Each charge value, represented with its error bar, corresponds to the mean value obtained from three experiments.

FM-MICP and FM-NICP voltammograms prove the incorporation of ATZ molecules into the matrixes of each molecularly imprinted conducting polymer, whatever the FM functional monomer. When present, ATZ molecules affect the conformation, the conductivity, and then the electrochemical signature of the electrosynthesized polymers.

The electroactivity of FM-NICP films is always higher than that of FM-MICP layers, as observed for TMA and Th (Figure 3A and B). The decrease in the charge passed in the FM-MICP voltammograms is due to ATZ molecules which induce conformational strain in the imprinted films upon oxidation. Due to the hindrance exercised by the presence of ATZ molecules, the conjugation length over the FM-MICP macromolecular chains is reduced, which modifies the electrochemical behavior^{17,18} as well as the optical properties^{19–22} of the conducting polymer based films.

Nevertheless, the observed difference between FM-MICP and FM-NICP voltammograms is more or less important depending on the nature of the FM. In particular, the difference is more pronounced in the case of TMA than in the case of the Th functional monomer (Figure 3). This demonstrates that the quantity of ATZ incorporated into the FM-MICP depends on the nature of the FM functional monomer and thus on the strength of the intermolecular interaction between ATZ and FM in the prepolymerization complex.

In order to quantify the relative difference between FM-MICP and FM-NICP voltammograms (due to the amount of incorporated ATZ molecules) for each FM functional monomer, electrooxidation charges are calculated, from cyclic voltammograms by area integration under the curves of current versus time. Charges $Q_{\text{FM-NICP}}$ and $Q_{\text{FM-MICP}}$ are first calculated from the FM-NICP and FM-MICP voltammograms, respectively. Then, a relative variation of the electrooxidation charge, Q_{FM} , is deduced from eq 1:

$$Q_{\text{FM}} = \frac{Q_{\text{FM-NICP}} - Q_{\text{FM-MICP}}}{Q_{\text{FM-NICP}}} \quad (1)$$

The so-calculated Q_{FM} values are represented on the histogram of Figure 3C as a function of the nature of the FM functional monomer. Each value corresponds to a mean value obtained from three independent measurements. Besides, the uncertainty bars corresponding to each point were displayed on the graph. It appears that Q_{TMA} is a little bit higher than Q_{TAA} , these two values being higher than Q_{TMeOH} and much higher than Q_{EDOT} and Q_{Th} .

These results indicate a decreased amount of incorporated ATZ molecules in the following order of functional monomers-based MICP: TMA, TAA, TMeOH, EDOT, and Th. Since a higher interaction between ATZ and FM functional monomer leads to a higher quantity of FM/ATZ prepolymerization complexes and to a better incorporation of ATZ into the FM-MICP polymerized matrix, one can suppose, at this stage of the work, that the noncovalent interactions between TMA and ATZ or between TAA and ATZ are stronger than the interactions involving TMeOH and much stronger than those implying EDOT and Th.

Note that in all the cases, for each FM-MICP electrosynthesis, EDOT is always present as a linker. As a consequence, since EDOT interacts (even weakly) with ATZ, EDOT/ATZ prepolymerization dimers are also to be considered. Thus, the embedded quantity of ATZ into the FM-MICP polymer matrix, in the cases of TMA, TAA, TMeOH, and Th, depends not only

on the FM/ATZ complex concentration but also on the EDOT/ATZ dimer number. However, in the case of EDOT-MICP, where EDOT plays the double role of linker and functional monomer, only the EDOT/ATZ complex quantity intervenes. Nevertheless, whatever the electrosynthesized FM-MICP, the study of the correlation between the Q_{FM} charge and the sum of the prepolymerization dimer concentrations, $[\text{FM}/\text{ATZ}] + [\text{EDOT}/\text{ATZ}]$, seems to be interesting. This will be considered in section 4.

2.5. FM-MICP Sensing Properties. Unlike nonimprinted conducting FM-NICP films, molecularly imprinted FM-MICP layers were electrosynthesized in the presence of atrazine. In order to quantitatively remove the target molecules from FM-MICP matrixes, a methanol/acetic acid solution was used to wash the polymer-coated electrodes. After this washing step, the obtained FM-MICP cyclic voltammograms were recorded for each FM functional monomer at the same scan rate of 25 mV s⁻¹. For illustration, Figure 4A and B (curve a) display the voltammograms obtained, respectively, in the cases of TMA and Th functional monomers. This washing step leads to the desired creation of free molecular imprinted cavities within the FM-MICP polymer matrixes, dedicated to the specific detection of additional ATZ molecules thanks to the establishment of new intermolecular FM/ATZ interactions between the probe-functionalized monomer units and the target molecules.

In order to check, for each kind of FM functional monomers, whether washed FM-MICP films are able to detect newly added target molecules, the modified gold electrodes were immersed in ACN solutions containing 0.1 mol L⁻¹ LiClO₄. Then, 10⁻⁴ mol L⁻¹ ATZ was added to the electrolytic solution. This quantity was much lower than that used for FM-MICP electrosynthesis (1.5 × 10⁻² mol L⁻¹). Cyclic voltammetry was then used at a scan rate of 25 mV s⁻¹ to check the modification of all FM-MICP voltammograms and to quantify the pesticide detection by the washed films. For illustration, Figure 4A and B (curve b) exhibit cyclic voltammograms of the previously studied washed TMA-MICP and Th-MICP (curve a) after the addition of 10⁻⁴ mol L⁻¹ in ATZ.

In the electrolytic medium, all the washed FM-MICP display a higher electroactivity in the absence of atrazine as observed for TMA and Th (Figure 4A and B). Such a decrease in current, observed when atrazine is added to the solution, can be attributed once again to the interaction of ATZ molecules with FM functional monomers into the polymer matrixes.^{12–14} Indeed, in the presence of ATZ, the electrooxidation of the polymer, which imposes the coplanarization of the chains, becomes much more difficult. Thus, a bigger quantity of detected targets induces a more important decrease in redox currents. These considerations indicate that a quantitative characterization of atrazine can be obtained from the analysis of the redox currents (or the involved redox charges) as a function of the concentration of atrazine in the analyzed solution.

The observed difference between FM-MICP voltammograms before and after addition of ATZ is more or less important depending on the nature of FM. In particular, this difference is more pronounced in the case of TMA than in the case of Th functional monomer (Figure 4). This demonstrates that the quantity of ATZ detected by the FM-MICP films depends on the nature of the FM functional monomer.

In order to quantify the current modification due to the detection of ATZ target molecules by FM-MICP layers (for each FM functional monomer), electrooxidation charges are calculated from cyclic voltammograms. First, a charge $Q'_{\text{FM-MICP}}$ is

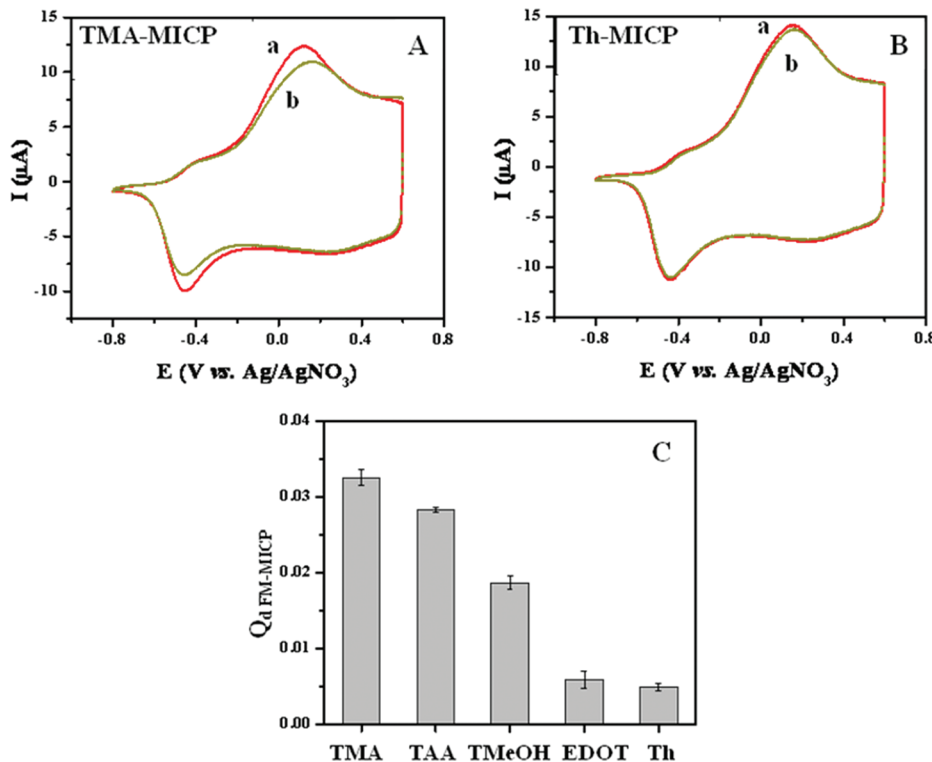


Figure 4. (A) Cyclic voltammograms of washed TMA-MICP (a) before and (b) after addition of 10^{-4} mol L^{-1} in ATZ. (B) Cyclic voltammograms of washed Th-MICP (a) before and (b) after addition of 10^{-4} mol L^{-1} in ATZ. All cyclic voltammograms were recorded in 0.1 M LiClO₄/ACN solutions at a scan rate of 25 mV s⁻¹. (C) Relative charges, Q_d FM-MICP, corresponding to ATZ detection by the different FM-MICP films (FM = TMA, TAA, TMeOH, EDOT, or Th). Each charge value, represented with its error bar, corresponds to the mean value obtained from three experiments.

calculated for the washed FM-MICP in the absence of any target molecule; second, a charge $Q''_{FM\text{-MICP}}$ is calculated for the FM-MICP in the presence of additional ATZ molecules. Finally, a relative “detection” charge can be calculated according to eq 2:

$$Q_d \text{ FM-MICP} = \frac{Q'_{FM\text{-MICP}} - Q''_{FM\text{-MICP}}}{Q'_{FM\text{-MICP}}} \quad (2)$$

Such a relative detection charge depends, as previously demonstrated, on the ATZ amount associated with the FM-MICP polymer matrix and must obviously be linked to the sensing properties of the conducting polymers. A better recognition of the target molecules by the sensing layer induces a higher value of Q_d FM-MICP.

The so-calculated Q_d FM-MICP values are represented on the histogram of Figure 4C as a function of the nature of FM functional monomer. Each point corresponds to a mean value obtained from three independent measurements. Besides, the uncertainty bars corresponding to each point were displayed on the graph. It appears that Q_d TMA-MICP and Q_d TAA-MICP are higher than Q_d TMeOH-MICP and much higher than Q_d EDOT-MICP and Q_d Th-MICP. These results indicate a decreased amount of detected ATZ molecules in the following order of functional monomers-based MICP: TMA, TAA, TMeOH, EDOT, and Th.

One can note that the dependence of Q_d FM-MICP (which reflects the target detection quality) with the nature of FM parallels that of Q_{FM} (which reflects the FM-MICP preparation quality). This can be explained as follows:

- A stronger interaction between ATZ and FM functional monomer in the FM/ATZ prepolymerization complex

leads to a better incorporation of ATZ into the electro-synthesized FM-MICP matrix, leading to a higher Q_{FM} value. This latter is then expected to increase with increasing concentrations of FM/ATZ prepolymerization complexes (in addition to EDOT/ATZ dimers as already discussed). Considering the different Q_{FM} experimental values, the noncovalent interactions between TMA and ATZ or between TAA and ATZ seem to be stronger than those involving TMeOH and much stronger than those implying EDOT and Th.

- Since the amount of incorporated ATZ molecules depends on the functional monomer used, one can suppose that the quantitative extraction of ATZ leads, in the washed FM-MICP matrixes, to a number of molecular imprints which also depends on the nature of FM. In particular, washed TMA-MICP and TAA-MICP should contain a higher number of functionalized cavities dedicated to ATZ detection.
- The strength of the interaction between ATZ and FM in the FM/ATZ prepolymerization complex should vary similarly to that between ATZ and FM in the FM-MICP polymer matrix. As a consequence, the sensing properties of washed FM-MICP layers do not depend only on the number of molecular imprints but also on the FM ability to interact with ATZ. Then, TMA-MICP and TAA-MICP, which contain a high number of imprints and which are also built from TMA and TAA functional monomers (that seem to strongly interact with ATZ), are characterized by great sensing properties toward ATZ, as traduced by the high corresponding experimental Q_d TMA-MICP and Q_d TAA-MICP values.

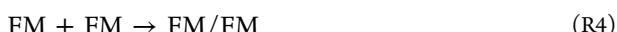
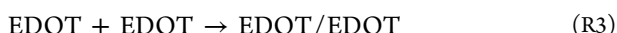
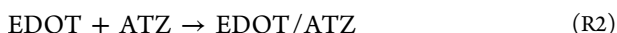
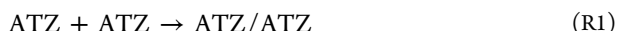
Note that in all the cases, for each FM-MICP electrosynthesis, EDOT is present as a linker. As a consequence, since EDOT interacts with ATZ and since EDOT/ATZ prepolymerization complexes are to be considered, the number of functionalized cavities into the FM-MICP polymer matrix, in the cases of TMA, TAA, TMeOH, and Th, depends also on the EDOT/ATZ dimer quantity (in addition to the FM/ATZ complex number). On another hand, when considering sensing properties of washed FM-MICP toward additional amounts of ATZ, EDOT-ATZ interactions must be considered in addition to FM-ATZ intermolecular bonds. As a consequence, whatever the electrosynthesized FM-MICP, the study of the correlation between the $Q_{d\text{ FM-MICP}}$ charge and the sum of the prepolymerization dimer concentrations, $[\text{FM}/\text{ATZ}] + [\text{EDOT}/\text{ATZ}]$, is very interesting. This will also be considered in section 4.

3. CALCULATION OF THE ASSOCIATION FREE ENERGIES IN SOLUTION

We demonstrated, in section 2, the clear effect of the nature of FM functional monomer, first, on the creation of ATZ molecular imprints into the polymer matrixes (through the Q_{FM} values) and, second, on the specific detection of ATZ targets (through the $Q_{d\text{ FM-MICP}}$ values). The obtained results were attributed to the strength of FM-ATZ interaction and then to the concentration of FM/ATZ (in addition to EDOT/ATZ) prepolymerization complexes.

For investigating this hypothesis and in order to check whether Q_{FM} and $Q_{d\text{ FM-MICP}}$ values are correlated with the sum of dimer concentrations, $[\text{FM}/\text{ATZ}] + [\text{EDOT}/\text{ATZ}]$, we need to determine the effective concentrations of the different prepolymerization complexes present in the medium before each FM-MICP electrosynthesis.

For this purpose, we calculate in the present section the free energies of the following six competitive reactions:



These reactions R1–R6, involved during FM-MICP preparation, are to be considered for each of the FM functional monomers. However, during EDOT-MICP synthesis, the EDOT molecule alone is associated with the ATZ, in the absence of any other FM functional monomer. Then, in the case of EDOT, only the first three reactions R1–R3 must be considered. Nevertheless, all these reactions are association reactions of the type



where sol means that the reaction takes place in solution in acetonitrile.

We have used the PCM (polarized continuum medium) method²³ within the SMD formalism,²⁴ available in the last version of the Gaussian code.²⁵ The PCM method is basically a method for calculating solvation free energies.²³ The SMD variant has been parametrized, so as to reproduce the standard

solvation free energies, $\Delta G_{\text{solv}}^{\circ}$, of a large list of molecules and ions in several solvents,²⁴ according to the formula

$$\Delta G_{\text{solv}}^{\circ\text{smd}}(\text{A}) = \Delta G_{\text{solv}}^{\text{smd}}(\text{A}) + RT \ln 24.5 \quad (3)$$

where $\Delta G_{\text{solv}}^{\text{smd}}(\text{A})$ is the simple difference of the quantum energies of one molecule in the vacuum and in the SMD cavity, which can be transposed to 1 mol L⁻¹ systems of a perfect gas and an ideal solution:

$$\Delta G_{\text{solv}}^{\text{smd}}(\text{A}) = G_{\text{sol}}^{\text{smd}}(\text{A}, 1 \text{ M}) - G_{\text{g}}(\text{A}, 1 \text{ M}) \quad (4)$$

The last term of eq 3 accounts for the different standard states in the gas phase (1 atm, concentration 1/24.5 mol L⁻¹) and in solution (concentration 1 mol L⁻¹).²⁶ In consequence, addressing reaction R7 leads to considering the thermodynamic cycle of Figure 5. From Figure 5 and eq 3, the free energy change of reaction R7 in solution reads

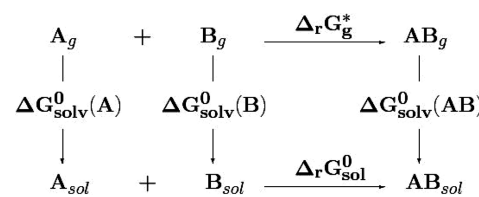


Figure 5. Thermodynamical cycle used for the calculation of the association free energies.

$$\begin{aligned} \Delta_r G_{\text{sol}}^{\circ\text{smd}} &= \Delta_r G_{\text{g}}^* + \Delta G_{\text{solv}}^{\circ\text{smd}}(\text{AB}) - \Delta G_{\text{solv}}^{\circ\text{smd}}(\text{A}) \\ &\quad - \Delta G_{\text{solv}}^{\circ\text{smd}}(\text{B}) \\ &= \Delta_r G_{\text{g}}^* + \Delta G_{\text{solv}}^{\text{smd}}(\text{AB}) - \Delta G_{\text{solv}}^{\text{smd}}(\text{A}) \\ &\quad - \Delta G_{\text{solv}}^{\text{smd}}(\text{B}) - RT \ln 24.5 \end{aligned} \quad (5)$$

where $\Delta_r G_{\text{g}}^*$ is the standard reaction free energy in the gas phase and $\Delta_r G_{\text{solv}}^{\circ\text{smd}}$ the SMD value of the standard reaction free energy in solution.

3.1. Free Energy Change in the Vacuum. Recent DFT calculations on oligothiophenes have emphasized the importance of long-range interactions.²⁷ In our case, this issue is still more important because of the formation of H bonded dimers: it is well-known that DFT calculations cannot describe van der Waals complexes, unless dispersion is taken into account and BSSE (basis set superposition error) is corrected. We have thus used the B97D functional, which includes the dispersion interactions,²⁸ and the SDD core pseudopotentials and basis sets,²⁹ supplemented with one d polarization Gaussians on all heavy atoms (exponents: 0.8 for C, N, and O atoms, 0.65 for S atoms, and 0.7 for Cl atoms). All the calculations have been done with the Gaussian 09 package.²⁵ Since we expect that in our dimers the leading interactions are hydrogen bond and π stacking, we have calculated the dimerization energies of benzene (C_6H_6), where π stacking is essential, and of water (H_2O), where hydrogen bond is predominant. For the benzene dimer, we have obtained for the dimerization energy the value 2.05 kcal mol⁻¹, to be compared with the CCSD(T) value 2.6 kcal mol⁻¹.³⁰ Our value is reasonable, though underestimated.

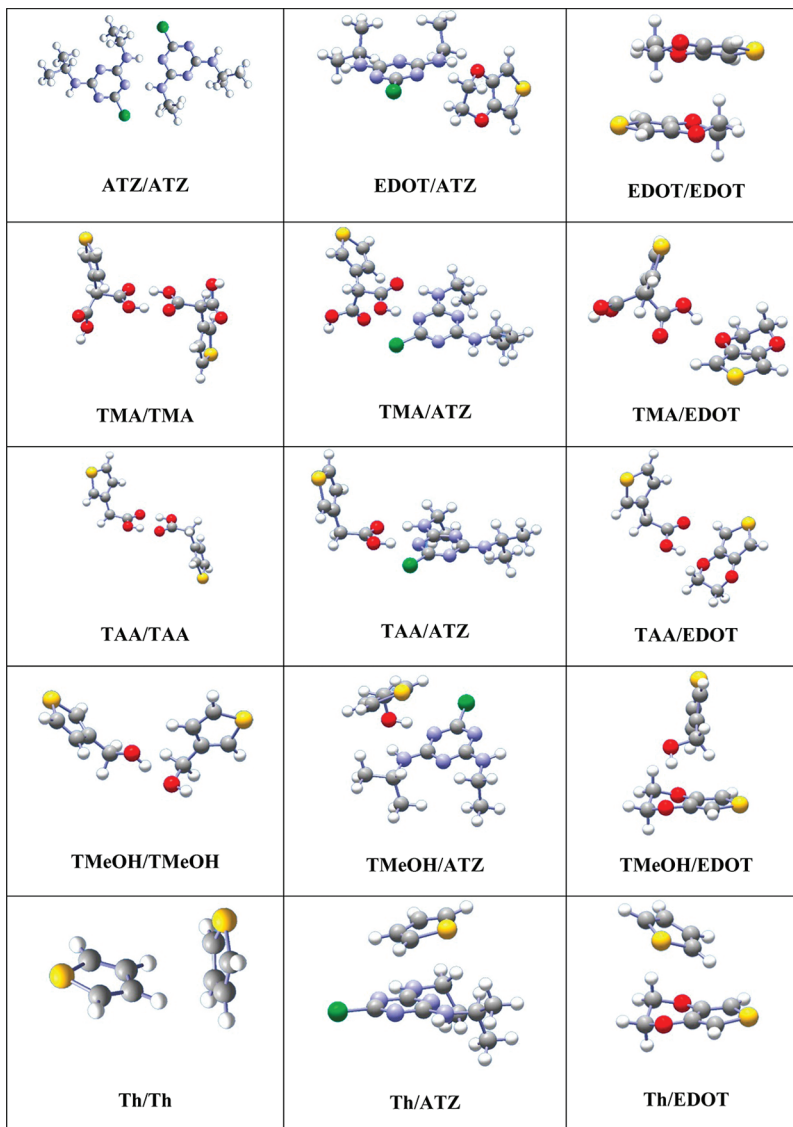


Figure 6. The dimers of atrazine (ATZ) and the different FM functional monomers (TMA, TAA, TMeOH, EDOT, and Th).

For the water dimer, we have obtained the value $5.53 \text{ kcal mol}^{-1}$, to be compared with the experimental value $5.44 \text{ kcal mol}^{-1}$.³¹ Our description of the hydrogen bond is excellent, therefore.

The structures of the dimers of interest are shown in Figure 6. Most dimers are linked by one or two hydrogen bonds, and those of thiophene, by π stacking. The bonding modes are given in Table 2. It can be seen that the atrazine molecule links to itself by a double H bond, to EDOT by a single H bond, to TAA and TMA by a double H bond, to TMeOH by both H bonding and π stacking, and to Th by π stacking only.

The translation, rotation, and vibration contributions to entropy have been calculated in the usual way with the help of the Sackur–Tetrode formula, of the rigid rotor and harmonic analysis, respectively.³² The $\Delta_r G_g^*$ values obtained in this way are given in Table 3 and shown in Figure 7 (“in the vacuum” entry). In every case, we have performed an extensive investigation of the possible energy minima. We found out that in most cases one single minimum is more stable than the other ones by 0.1 eV or more, so that the secondary minima can be neglected. In a few cases, we have found several minima with very close energies. This is the case, for instance, for the

EDOT/ATZ case where we found two structures, with the H bonding to EDOT on the ethyl vs the isopropyl side yielding very close free energies (+0.056 and +0.059 eV, respectively). In these cases, we have considered these structures equivalent and added $R \ln 2$ to the conformation entropy.

It can be seen in Figure 7 that the double H bond is the most efficient bonding mode with very negative $\Delta_r G_g^*$ values: ATZ/ATZ (-0.21 eV), TAA/ATZ (-0.23 eV), TAA/TAA (-0.20 eV), TMA/ATZ (-0.26 eV). The single H bond is less efficient with slightly positive $\Delta_r G_g^*$ values: EDOT/ATZ (+0.056 eV), TAA/EDOT (+0.079 eV), TMeOH/TMeOH (+0.043 eV). The π stacking binding mode yields very unfavorable binding free energies: Th/ATZ (+0.191 eV). Note that the values of Table 3 are free from the conformation entropy. This effect has been discussed in the literature; see the work of Mammen.³³ Considering the present list of monomers (Figure 1) and dimers (Figure 6), conformation entropy can originate from the following features:

- (1) The free or partially restricted rotation of some substituents of the monomers may become more restricted in the dimer. This question arises mainly for the ethyl

Table 2. Conformation Entropy for the Formation of Dimers and Its Contribution to Free Energy^a

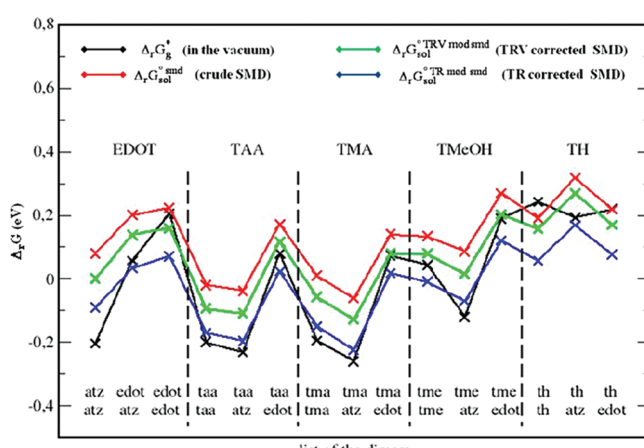
	bonding mode	conformation effects	conformation entropy	contribution to free energy (eV)
ATZ/ATZ	double H bond	C and T conformers of ATZ	+R ln(16/9)	-0.015
EDOT/ATZ	H bond	C and T conformers of ATZ	+R ln(16/3)	-0.043
EDOT/EDOT	dipole-dipole	a/b stacking	+R ln 4	-0.036
TMA/ATZ	double H bond	C and T conformers of ATZ + two COOH on TMA	+R ln(8/3)	-0.025
TMA/TMA	double H bond	two COOH on TMA	+R ln 4	-0.036
TMA/EDOT	H bond	two O on EDOT + two COOH on TMA	+R ln 4	-0.036
TAAT/ATZ	double H bond	C and T conformers of ATZ	+R ln(4/3)	-0.007
TAAT/TAAT	double H bond		0	0
TAAT/EDOT	H bond	two O on EDOT	+R ln 2	-0.018
TMeOH/ATZ	double H bond + π stacking	C and T conformers of ATZ + a/b stacking	+R ln(8/3)	-0.025
TMeOH/TMeOH	H bond	donor vs acceptor H bond	+R ln 2	-0.018
TMeOH/EDOT	H bond + π stacking	two O on EDOT + a/b stacking	+R ln 4	-0.036
Th/ATZ	π stacking	a/b and l/r stackings	+R ln 4	-0.036
Th/Th	π stacking	a/b and l/r stackings	+R ln 4	-0.036
Th/EDOT	π stacking	a/b and l/r stackings	+R ln 4	-0.036

^aa/b and l/r stand for the above/below and left/right alternatives.

Table 3. Formation Free Energies ($\Delta_f G_g^*$, $\Delta_f G_{\text{sol}}^{\text{smd}}$, $\Delta_f G_{\text{sol}}^{\text{oTRV mod smd}}$, and $\Delta_f G_{\text{sol}}^{\text{oTR mod smd}}$) and Solvation Free Energies in Acetonitrile (ΔG_{solv}) of the Different Dimers of Interest (in eV)^a

	$\Delta_f G_g^*$	ΔG_{solv}	$\Delta_f G_{\text{sol}}^{\text{smd}}$	$\Delta_f G_{\text{sol}}^{\text{oTRV mod smd}}$	$\Delta_f G_{\text{sol}}^{\text{oTR mod smd}}$
ATZ/ATZ	-0.205	-1.25	+0.079	-0.001	-0.092
EDOT/ATZ	+0.056	-0.907	+0.193	+0.130	+0.033
EDOT/EDOT	+0.204	-0.536	+0.222	+0.158	+0.070
TMA/ATZ	-0.261	-1.106	-0.062	-0.129	-0.225
TMA/TMA	-0.196	-0.872	+0.008	-0.058	-0.151
TMA/EDOT	+0.072	-0.771	+0.139	+0.078	-0.017
TAAT/ATZ	-0.232	-0.942	-0.039	-0.110	-0.197
TAAT/TAAT	-0.201	-0.556	-0.021	-0.095	-0.172
TAAT/EDOT	+0.079	-0.599	+0.170	+0.116	+0.021
TMeOH/ATZ	-0.121	-0.884	+0.085	+0.013	-0.071
TMeOH/TMeOH	+0.043	-0.556	+0.133	+0.078	-0.010
TMeOH/EDOT	+0.188	-0.520	+0.268	+0.202	+0.120
Th/ATZ	+0.191	-0.799	+0.317	+0.267	+0.168
Th/Th	+0.241	-0.367	+0.190	+0.157	+0.056
Th/EDOT	+0.218	-0.431	+0.217	+0.168	+0.075

^aT, R, and V allude to the translation, rotation, and vibration of the molecules in the vacuum. In this table, the conformation entropies of Table 2 are not taken into account.

Figure 7. Dimerization free energies ($\Delta_f G_g^*$, $\Delta_f G_{\text{sol}}^{\text{smd}}$, $\Delta_f G_{\text{sol}}^{\text{oTR mod smd}}$, and $\Delta_f G_{\text{sol}}^{\text{oTR mod smd}}$) obtained with several levels of approximation.

and isopropyl substituents of the ATZ molecule. We have considered that the rotation freedom of these groups is not modified by the dimer formation.

- (2) Some conformers of the monomers do not participate in the formation of dimers.
- (3) Several equivalent but distinct structures may exist. In this case, we add to the entropy the term $R \ln N$, where N is the number of distinct structures. For example, in the case of π stacking of two molecules, one molecule can stack above or below the other one. In this case, we add $R \ln 2$ to the entropy.

We now investigate the dimerization of the ATZ molecule in some detail. If we first consider the ATZ molecule, the following points can be noted:

- (1) The monomer has two sides, and each of them can be cis (C) or trans (T); see Figure 1 showing one of the ATZ conformers. If we note Ce, Ci, Te, and Ti the C and T sides of ATZ bearing the ethyl and isopropyl groups,

- respectively, then the ATZ molecule displays four distinct conformers: CeCi, CeTi, CiTe, and TeTi. With these notations, Figure 1 shows the CeTi conformer of ATZ. The CeCi and TeTi conformers can be simply noted CC and TT.
- (2) We have calculated that, in solution, the TT conformer is the most stable, that the CeTi and CiTe conformers lie higher but within 0.02 eV only, and that the CC conformer lies 0.05 eV higher than TT. Considering that kT amounts to 0.025 eV (at 300 K), we conclude that three conformers (TT, CeTi, and CiTe) can be considered degenerate and that the fourth one (CC) can be neglected.
 - (3) Since each monomer has three accessible conformers, the conformation entropy of a pair of separated monomers amounts to $+R \ln 9$.

We now note that in the dimer:

- (1) The monomers are linked through a double H bond between their T sides. We have verified that binding the C sides leads to dimers with energies higher by at least 0.10 eV.
- (2) The Ti and Te sides of each monomer are no more equivalent, so that the number of different dimers amounts to $4 \times 4 = 16$ and the conformation entropy amounts to $+R \ln 16$.

The conformation entropy of the ATZ dimerization is thus $\Delta S_{\text{conf}} = R \ln(16/9)$ and the corresponding free energy must be added the value $-RT \ln(16/9) = -0.015$ eV.

We have investigated the 14 other dimers in the same way. For the sake of concision, we only summarize our conclusions in Table 2, where we give the origins of conformation entropy and the corresponding contributions to dimerization entropies and free energies.

3.2. Free Energy Change in Solution: the PCM Paradox. We have calculated the solvation free energies, $\Delta G_{\text{solv}}^{\text{smd}}$, of all the monomers and dimers relevant to the present study. Since the Gaussian package enables the BSSE correction in the vacuum only, we have evaluated the solvation free energies of the dimers (Table 3) with a single point electronic calculation at the geometry optimized in the vacuum with BSSE correction. For the sake of consistency, we have also calculated the solvation free energies of the monomers (Table 4)

Table 4. Solvation Free Energies in Acetonitrile ($\Delta G_{\text{solv}}^{\text{smd}}$) of the Monomers of Interest (in eV)

	ATZ	TMA	TAA	TMeOH	EDOT	Th
$\Delta G_{\text{solv}}^{\text{smd}}$	-0.808	-0.579	-0.409	-0.364	-0.318	-0.194

with single point calculations at the geometries optimized in the vacuum.

The SMD solvation free energies can be written as²³

$$\Delta G_{\text{solv}}^{\text{smd}} = \Delta G_{\text{solv}}^{\text{electr}} + \Delta G_{\text{solv}}^{\text{nonelectr}} \quad (6)$$

The first term of eq 6, $\Delta G_{\text{solv}}^{\text{electr}}$, is the interaction energy of the solute with the polarized solvent, modeled by a homogeneous dielectric medium with the dielectric constant of the solvent. The second term of eq 6, $\Delta G_{\text{solv}}^{\text{nonelectr}}$, gathers the cavitation, dispersion, and Pauli repulsion effects.²³ Like most PCM methods, the SMD method uses atomic radii which have been optimized, so that the free energy of eq 3 reproduces the measured values of a list of molecules. Note that, from eq 6, the additivity of the solvation free energies is mainly ruled by electrostatic and cavitation effects.

The SMD values of the solvation free energies of the dimers $\Delta G_{\text{solv}}^{\text{smd}}$ and of the dimerization standard free energies, $\Delta_r G_{\text{sol}}^{\text{smd}}$, calculated according to eq 5, are given in Table 3 and shown in Figure 7 ("crude SMD" entries). It can be seen in Figure 7 that these crude SMD values are much more positive than the values in the vacuum, $\Delta_r G_g^*$.

We now emphasize that some terms are absent from eq 6. In the gas phase, the entropy of a molecule is usually separated in three components: translation, rotation, and vibration. These effects are certainly present in the $\Delta_r G_g^*$ term of eq 5. According to the Sackur–Tetrode formula, the translation entropy varies exactly like the logarithm of the mass (M) of the molecule.³² It has been noted that the rotation term roughly varies in the same manner.³³ This can be checked in Figure 8

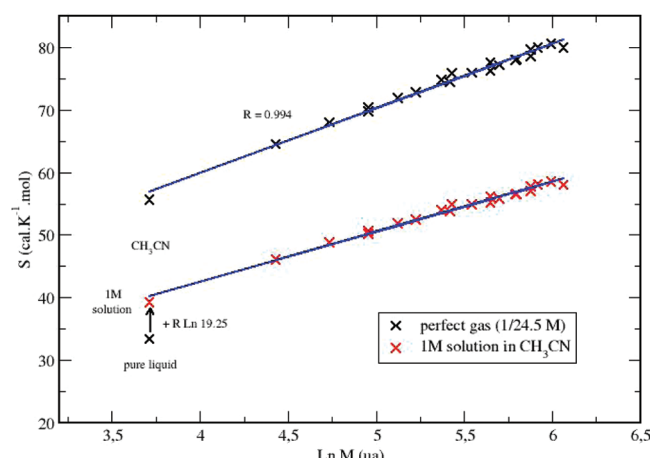


Figure 8. Entropy of the molecules of interest in the present work: translation rotation entropy in the gas phase and entropy deduced from the Wertz formula in solution.

where we have plotted the translation rotation entropies of all the molecules of present interest (monomers and dimers, and acetonitrile) in the gas phase against the logarithm of their mass. It can be seen that the correlation is quite good ($R = 0.994$). The question is now that the same effects, namely, translation and rotation in solution, and also other effects such as solute solvent conformation entropy, are absent from eq 6, at least formally.

We here face the PCM paradox: the atomic radii have been optimized, so that the method reproduces the solvation free energies of a list of molecules. In consequence, the above-mentioned entropy terms, lacking in the formalism, are numerically present in the PCM result.

We now understand that the SMD solvation free energies of the dimers are inaccurate. Actually, one part of the entropy of the $A + B \rightarrow AB$ reaction should vary like $\ln[(M_A + M_B)/(M_A M_B)]$; this is not enabled by the PCM equation (eq 6). The loss of rotational and translational entropy due to the fixation of a ligand to a molecule has been discussed in the literature for a long time.^{33–35} We decided to introduce an empirical correction to the solvation free energies, with a realistic mass dependence. Of course, we know that, doing so, we lose the good accuracy of the solvation free energies of the monomers given in Table 4, but we expect that their additive behavior will be improved and the dimerization free energies as well.

3.3. Empirical Treatment of Solute Entropies. We used the empirical formula given by D. Wertz in 1980.³⁶ Since 1980, the Wertz formula has been both severely criticized³⁷ and

empirically used with success.^{38–43} D. Wertz noticed that the relative entropy loss of a molecule passing from the gas phase to the solution does not depend on the molecule, and that consequently it can be taken in the solvent molecule itself.

We used the available values of the standard molar entropy of liquid acetonitrile, 35.76 cal K⁻¹ mol⁻¹ at 298.15 °C,⁴⁴ and calculated the gas phase value with the help of the Sackur–Tetrode, harmonic analysis, and rigid rotor formulas for translation, vibration, and rotation, respectively.²⁵ This yielded the value 58.0 cal K⁻¹ mol⁻¹ at 298.15 °C, in excellent agreement with the measured value: 58.2 cal K⁻¹ mol⁻¹.⁴⁴ According to D. Wertz, this gas phase entropy must be brought to the standard state of the pure liquid, for which the concentration has the value 19.25 mol L⁻¹.⁴⁵ The total gas phase entropy now amounts to

$$\begin{aligned} S_g^{\text{TRV}}(19.25 \text{ M}) &= 58.0 - R \ln(24.5 \times 19.25) \\ &= 58.0 - 12.24 \\ &= 45.7 \text{ cal K}^{-1} \text{ mol}^{-1} \end{aligned} \quad (7)$$

From these numbers, we can deduce that for acetonitrile

$$\frac{S_g^{\text{TRV}}(19.25 \text{ M}) - S_{\text{sol}}^{\text{tot}}(19.25 \text{ M})}{S_g^{\text{TRV}}(19.25 \text{ M})} = 0.22 \quad (8)$$

In eqs 7 and 8, the total entropy is noted S_g^{TRV} (TRV for translation rotation vibration) in the gas phase and $S_{\text{sol}}^{\text{tot}}$ (tot for total) in the solution. According to Wertz, eq 8, exact for acetonitrile, can be used for any solute in acetonitrile and can be readily exploited with the help of the thermodynamic cycle of Figure 9.³⁶ On this cycle, we use two intermediate states of

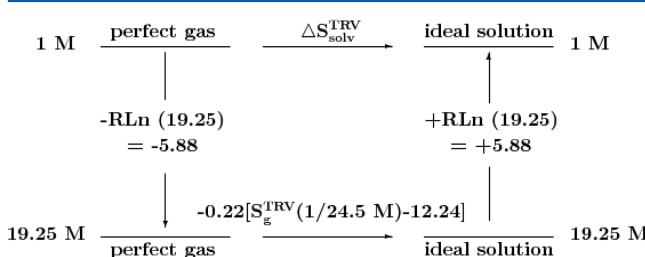


Figure 9. The thermodynamic cycle used for the Wertz formula in acetonitrile.

the solute: first a 1 mol L⁻¹ perfect gas is compressed to a hypothetical 19.25 mol L⁻¹ perfect gas state, then solvated in a hypothetical 19.25 mol L⁻¹ ideal solution state, and eventually diluted to a 1 mol L⁻¹ ideal solution. Using this cycle, we obtain (in cal K⁻¹ mol⁻¹)

$$\begin{aligned} \Delta S_{\text{solv}}^{\text{TRV}} &= S_{\text{sol}}^{\text{tot}}(1 \text{ M}) - S_g^{\text{TRV}}(1 \text{ M}) \\ &= -5.88 - 0.22(S_g^{\text{TRV}}(1/24.5 \text{ M}) \\ &\quad - 12.24) + 5.88 \\ &= -0.22(S_g^{\text{TRV}}(1/24.5 \text{ M}) - 12.24) \end{aligned} \quad (9)$$

We now modify the SMD solvation free energies:

$$\Delta G_{\text{solv}}^{\text{TRV mod smd}} = \Delta G_{\text{solv}}^{\text{smd}} - T \Delta S_{\text{solv}}^{\text{TRV}} \quad (10)$$

and, eventually, the dimerization free energy for reaction R7:

$$\begin{aligned} \Delta_r G_{\text{sol}}^{\circ \text{TRV mod smd}} &= \Delta_r G_g^* + \Delta G_{\text{solv}}^{\text{TRV mod smd}}(\text{AB}) \\ &\quad - \Delta G_{\text{solv}}^{\text{TRV mod smd}}(\text{A}) - \Delta G_{\text{solv}}^{\text{TRV mod smd}}(\text{B}) \\ &\quad - RT \ln 24.5 \end{aligned} \quad (11)$$

We have then considered that the Wertz formula is best justified when applied to only the translation rotation part of the entropy. We here intuitively consider that, due to the potential created by the solvent, the densities of states for the translation and rotation of the solute do decrease but the density of internal vibration states of the solute is not affected. In consequence, we subtract the harmonic analysis entropies of acetonitrile in the vacuum and, for the sake of consistency, in the PCM cavity as well:²⁵

$$\begin{aligned} S_g^{\text{TR}}(19.25 \text{ M}) &= 45.70 - 2.41 \\ &= 43.30 \text{ cal K}^{-1} \text{ mol}^{-1} \end{aligned} \quad (12)$$

$$\begin{aligned} S_{\text{sol}}^{\text{tot-V}}(19.25 \text{ M}) &= 35.76 - 2.35 \\ &= 33.40 \text{ cal K}^{-1} \text{ mol}^{-1} \end{aligned} \quad (13)$$

where S_g^{TR} is the translation rotation entropy in the gas phase and where $S_{\text{sol}}^{\text{tot-V}}$ is the corresponding entropy in the solution (tot-V for “total, minus internal vibration”) because in solution not only two but several effects remain: translation, rotation, solute–solvent vibration, and conformation entropies. With these new values, we obtain

$$\frac{S_g^{\text{TR}}(19.25 \text{ M}) - S_{\text{sol}}^{\text{tot-V}}(19.25 \text{ M})}{S_g^{\text{TR}}(19.25 \text{ M})} = 0.23 \quad (14)$$

and finally, in full analogy with eqs 9, 10, and 11,

$$\begin{aligned} \Delta S_{\text{solv}}^{\text{TR}} &= S_{\text{sol}}^{\text{tot-V}}(1 \text{ M}) - S_g^{\text{TR}}(1 \text{ M}) \\ &= -0.23(S_g^{\text{TR}}(1/24.5 \text{ M}) - 12.24) \end{aligned} \quad (15)$$

$$\Delta G_{\text{solv}}^{\text{TR mod smd}} = \Delta G_{\text{solv}}^{\text{smd}} - T \Delta S_{\text{solv}}^{\text{TR}} \quad (16)$$

$$\begin{aligned} \Delta_r G_{\text{sol}}^{\circ \text{TR mod smd}} &= \Delta_r G_g^* + \Delta G_{\text{solv}}^{\text{TR mod smd}}(\text{AB}) \\ &\quad - \Delta G_{\text{solv}}^{\text{TR mod smd}}(\text{A}) - \Delta G_{\text{solv}}^{\text{TR mod smd}}(\text{B}) \\ &\quad - RT \ln 24.5 \end{aligned} \quad (17)$$

As stated at the end of section 3.2, eqs 10 and 16 certainly deteriorate the SMD values of the solvation free energies of the monomers, but we expect that the dimerization free energies will be improved. We have used the two possibilities, using the total (TRV, from eq 11) and reduced (TR, from eq 17) values of the entropy in the gas phase. The corresponding values of the dimerization free energies, $\Delta_r G_{\text{sol}}^{\circ \text{TRV mod smd}}$ and $\Delta_r G_{\text{sol}}^{\circ \text{TR mod smd}}$, are given in Table 3 and shown in Figure 7 (“TRV” and “TR corrected SMD” entries). It can be seen that the two ways of correcting the solvation entropy make the association free energies much more negative than the SMD values ($\Delta_r G_{\text{sol}}^{\circ \text{smd}}$) and that dropping the vibration entropy from the empirical treatment (TR correction) yields the

largest correction. These results can be understood in the following way:

- (1) The sign of the TR correction can be easily predicted. From eqs 15, 16, and 17, we can write

$$\begin{aligned} \Delta_r G_{\text{sol}}^{\circ \text{TR mod smd}} &= \Delta_r G_{\text{sol}}^{\circ \text{smd}} + 0.23T(S_g^{\text{TR}}(\text{AB}) - S_g^{\text{TR}}(\text{A}) \\ &\quad - S_g^{\text{TR}}(\text{B}) + 12.24) \end{aligned} \quad (18)$$

- From Figure 8, it is seen that, due to the small variation of the gas phase entropies with the mass M of the molecule, the second term of eq 18 is always negative.
- (2) Concerning the TRV modification of the free energies, an equation similar to eq 18 can be written from eqs 9, 10, and 11:

$$\begin{aligned} \Delta_r G_{\text{sol}}^{\circ \text{TRV mod smd}} &= \Delta_r G_{\text{sol}}^{\circ \text{smd}} + 0.22T(S_g^{\text{TRV}}(\text{AB}) \\ &\quad - S_g^{\text{TRV}}(\text{A}) - S_g^{\text{TRV}}(\text{B}) + 12.24) \end{aligned} \quad (19)$$

which can be written, thanks to the additivity of entropies in the gas phase, as

$$\begin{aligned} \Delta_r G_{\text{sol}}^{\circ \text{TRV mod smd}} &= \Delta_r G_{\text{sol}}^{\circ \text{TR mod smd}} + 0.22T \\ &\quad (S_g^{\text{V}}(\text{AB}) - S_g^{\text{V}}(\text{A}) - S_g^{\text{V}}(\text{B}) + 12.24) \end{aligned} \quad (20)$$

where $S_g^{\text{V}}(\text{A})$ is the vibrational entropy of A in the gas phase. We have found out that the vibrational correction to the free energies, second term of eq 20, is always positive. This is due to the fact that, unlike the translation rotation entropies, the vibrational entropies increase very rapidly with the mass of the molecules.

It is also striking that the TR correction yields values of the free energies rather close to the values in the vacuum. When passing from the gas phase to the solution, two effects modify the dimerization free energies:

- (1) The electrostatic stabilization of the dimers is smaller than that of the pair of the separated monomers. For example, it can be seen in Tables 3 and 4 that the solvation free energy of two separate ATZ monomers amounts to -1.6 eV and that the value for the ATZ/ATZ dimer amounts to -1.25 eV only. This effect yields a positive contribution to the dimerization free energies in solution.
- (2) As already mentioned, eq 18 shows that the TR correction to the SMD values is always negative.

The close results of the two approaches ("in the vacuum" and "TR modified SMD") show that these two effects roughly cancel out. Of course, this closeness of results is fortuitous because the two canceling effects depend on the nature of the solvent in different ways.

We have also verified that the correction to the reaction free energies depends on the mass of the molecules: for the lightest dimer Th/Th, the correction amounts to -0.13 eV; for the heaviest dimer ATZ/ATZ, it amounts to -0.17 eV. This is the order of magnitude given in ref 46 for the entropy barrier to the binding of ligands to molecules.

3.4. A Simple Test Case. The thermodynamic cycle of Figure 9 has been severely criticized,³⁷ but we emphasize that this cycle is actually correct, only the hypothetical states may be said unreasonable. The Wertz formula is empirical and, like any empirical formula, it can have fields of poor applicability and fields of good applicability. It is therefore important to show its pertinency in the present field of association reactions.

In this section, we test our two versions of the Wertz formula on an association reaction for which the free energy change has been accurately measured. This reaction is the following, taken in ref 40:



for which the value $\Delta_r G_{\text{sol}}^{\circ} = -4.2$ kcal/mol has been measured in water.⁴⁷ The authors of ref 40 have used the PB (Poisson–Boltzmann) version of the reaction field, together with the B3LYP functional²⁵ and the 6-311 g(d,p) basis set.²⁵ In this way, they get the reaction free energy -3.8 kcal/mol. The free energy of reaction R8 reads

$$\begin{aligned} \Delta_r G_{\text{sol}}^{\circ \text{mod smd}} &= \Delta_r G_g^* + \Delta G_{\text{solv}}^{\text{mod smd}}(\text{AB}) \\ &\quad - \Delta G_{\text{solv}}^{\text{mod smd}}(\text{A}) \\ &\quad - \Delta G_{\text{solv}}^{\text{mod smd}}(\text{B}) - RT \ln 24.5 \\ &\quad - RT \ln 55.5 \end{aligned} \quad (21)$$

where the last term accounts for the fact that, in reaction R8, the water is both reactant and solvent and where the solvation free energies are modified according to eqs 10 and 16 and with the Wertz formula in water:³⁶

$$\Delta S_{\text{solv}}(\text{A}) = -0.46(S_g(\text{A}) - 14.3) \quad (22)$$

We have calculated the free energy of reaction R8 with the B3LYP functional, the 6-311 g(d,p) basis like in ref 40. We have also used the SMD reaction field and the Wertz formula (eq 22). Our results are given in Table 5. It can be seen that

Table 5. Free Energy Change (in kcal/mol) of Reaction R8 with Our Methods

	in the vacuum	crude SMD	TRV corrected SMD	TR corrected SMD	experimental value
$\Delta_r G_{\text{sol}}^{\circ}$	+0.6	+0.3	-4.4	-4.0	-4.2

- (1) Our results are close to those of ref 40, calculated with the PB formalism.
- (2) The crude SMD value has the wrong sign and is too positive by 4.5 kcal/mol.
- (3) The Wertz formula dramatically improves the value of the reaction free energy. Both the TRV and TR corrected values are excellent and actually bracket the experimental value.

We conclude that the crude SMD method cannot be applied to association reactions such as reaction R8 and that the Wertz formula provides a simple and efficient correction to the reaction free energy. Since the dimerization reactions, reactions R1 to R6, are of the type $\text{A}_{\text{sol}} + \text{B}_{\text{sol}} \rightarrow \text{AB}_{\text{sol}}$, just like reaction R8, the present success of the Wertz formula makes us confident with the approach that we have proposed in section 3.3.

Table 6. Concentrations (in mol L⁻¹) of the FM/ATZ and EDOT/ATZ Prepolymerization Complexes (Corresponding to Each FM-MICP Preparation) Obtained with Different Treatments of the Free Energies (Thanks to $\Delta_r G_g^*$, $\Delta_r G_{sol}^{osmd}$, $\Delta_r G_{sol}^{TRV \text{ mod smd}}$, and $\Delta_r G_{sol}^{oTR \text{ mod smd}}$, Respectively)^a

		in the vacuum	crude SMD	TRV corrected SMD	TR corrected SMD
TMA-MICP	[TMA/ATZ]	0.14×10^{-1}	0.47×10^{-2}	0.11×10^{-1}	0.15×10^{-1}
	[EDOT/ATZ]	0.62×10^{-6}	0.91×10^{-7}	0.86×10^{-6}	0.88×10^{-6}
TAA-MICP	[TAA/ATZ]	0.11×10^{-1}	0.18×10^{-2}	0.73×10^{-2}	0.13×10^{-1}
	[EDOT/ATZ]	0.16×10^{-5}	0.13×10^{-6}	0.20×10^{-5}	0.31×10^{-5}
TMeOH-MICP	[TMeOH/ATZ]	0.49×10^{-2}	0.29×10^{-4}	0.45×10^{-3}	0.53×10^{-2}
	[EDOT/ATZ]	0.18×10^{-4}	0.15×10^{-6}	0.38×10^{-5}	0.12×10^{-4}
EDOT-MICP	[EDOT/ATZ]	0.16×10^{-4}	0.60×10^{-6}	0.20×10^{-4}	0.43×10^{-3}
Th-MICP	[Th/ATZ]	0.30×10^{-5}	0.12×10^{-6}	0.40×10^{-5}	0.38×10^{-4}
	[EDOT/ATZ]	0.19×10^{-4}	0.15×10^{-6}	0.40×10^{-5}	0.14×10^{-4}
R		0.983	0.809	0.910	0.992

^aR is the correlation coefficient between the sum ([FM/ATZ] + [EDOT/ATZ]) and the measured Q_{FM} electrochemical charge.

4. DFT RESULTS VERSUS ELECTROCHEMICAL MEASUREMENTS: A DISCUSSION

In this section, we deduce from the dimerization free energies the values of the concentrations of the different prepolymerization complexes present in the medium before each FM-MICP electrosynthesis. Since EDOT plays the same role as FM, we consider that the relevant quantity for the interpretation of the electrochemical results is the sum of the concentrations of the FM/ATZ and EDOT/ATZ dimers. We will therefore investigate whether the values of the Q_{FM} and Q_d FM-MICP signals are correlated with the sum of the concentrations: [FM/ATZ] + [EDOT/ATZ].

For a given FM functional monomer, different from EDOT, there are nine unknown quantities, the concentrations of the monomer and dimer species involved in the prepolymerization medium during FM-MICP preparation: ATZ, EDOT, FM, ATZ/ATZ, EDOT/ATZ, FM/ATZ, EDOT/EDOT, FM/EDOT, and FM/FM. These unknowns are solutions of a system of three linear equations (conservation of matter for the monomers) and six nonlinear equations (law of mass action for the six dimers). When only EDOT is used for EDOT-MICP preparation, with no other FM functional monomer, there are only five unknowns and five equations. We have solved these systems of equations for each functional monomer, with the help of our own code, based on random variations of the concentrations. We have used the following values of initial concentrations, given in section 2.2: $[ATZ]_0 = 1.5 \times 10^{-2}$ mol L⁻¹, $[EDOT]_0 = 7.5 \times 10^{-3}$ mol L⁻¹, and $[FM]_0 = 3 \times 10^{-2}$ mol L⁻¹. All the monomer and dimer concentrations have been determined according to the four different treatments of the free energies: in the vacuum ($\Delta_r G_g^*$ values) and in solution ($\Delta_r G_{sol}^{osmd}$, $\Delta_r G_{sol}^{TRV \text{ mod smd}}$, and $\Delta_r G_{sol}^{oTR \text{ mod smd}}$ values). The [FM/ATZ] and [EDOT/ATZ] concentrations involved during each FM-MICP preparation are given in Table 6.

We found out that for very negative free energies (say < -0.15 eV, TAA and TMA cases) the concentrations of the FM/ATZ dimers are close to their maximum value (1.5×10^{-2} mol L⁻¹, initial value of the ATZ concentration) and are almost insensitive to small variations of the free energies. This is also true for the most positive values of the free energies (say > +0.15 eV, Th and EDOT cases) for which the concentration of the FM/ATZ dimer is found close to zero.

On the other hand, when the free energy lies in between the extreme values (TMeOH case), we found that the dimer concentration is highly sensitive to small variations of the free energy, as small as 0.02 eV. This is the order of magnitude of

the conformation entropy. It has been noted that using simple rules of thumb, like that of section 3.1 and Table 2, we can overestimate the conformation entropy by a factor of 2.³³ For this reason, we worked in the following way:

- (1) We calculate the concentrations twice, with free energies including (c_y) and not including (c_n) the conformation entropies.
- (2) We adopt for the concentration half the sum of the two values:

$$c = \frac{c_y + c_n}{2} \quad (23)$$

- (3) We also consider that the difference provides us with a kind of error bar:

$$\Delta c = c_y - c_n \quad (24)$$

According to formulas 23 and 24, all the concentrations can be written as $c \pm \Delta c/2$. The [FM/ATZ] and [EDOT/ATZ] concentrations, calculated in this way, are given in Table 6. It can be seen that, in all cases but one (Th), the [EDOT/ATZ] concentrations are always much smaller than the [FM/ATZ] concentrations. In the case of Th, the contrary is obtained. This feature can be easily understood from Figure 7: in all cases but one (Th case), the value of the interaction free energy in the EDOT/ATZ dimer is more positive than the value for the FM/ATZ complex.

In Figures 10 and 11, we plot the experimental Q_{FM} charges against the sum of the dimer concentrations: [FM/ATZ] + [EDOT/ATZ] (calculated with the four sets of values of the free energies). It can be seen that:

- (1) The crude SMD values yield very small concentrations and a poor correlation ($R = 0.809$, Figure 10 top). Actually the free energies in the vacuum yield more reasonable values of the concentrations and a stronger correlation with experimental values ($R = 0.983$, Figure 10 top).
- (2) The TRV modified free energies yield a strong correlation between Q_{FM} charges and concentrations ($R = 0.910$, Figure 10 bottom).
- (3) The TR corrected SMD values yield the best correlation between the Q_{FM} charges and the dimer concentrations ($R = 0.992$, Figure 11 top).

The strongest correlation is thus yielded by the $\Delta_r G_{sol}^{oTR \text{ mod smd}}$ value, which has been discussed in section 3.3 to be the best

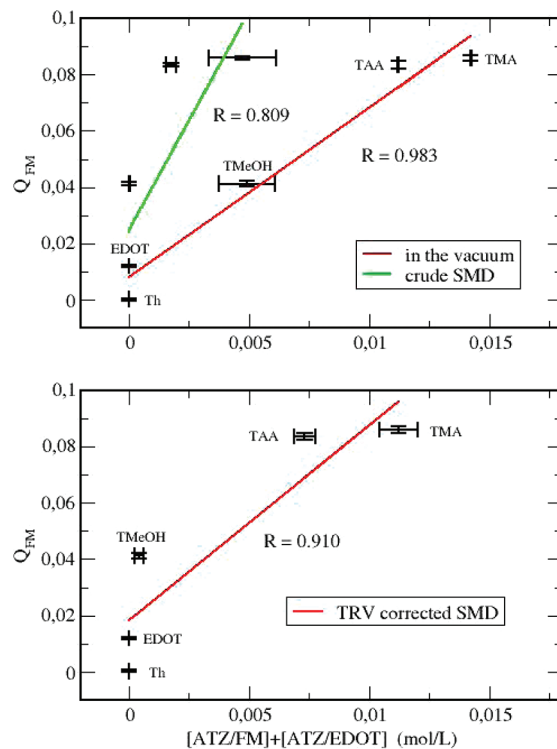


Figure 10. Correlation of the experimental Q_{FM} charge with the total concentration of ATZ heterodimers. Concentrations are obtained with different calculations of the dimerization free energies (top, $\Delta_r G_g^*$ and $\Delta_r G_{sol}^{osmd}$; bottom, $\Delta_r G_{sol}^{TRV \text{ mod } smd}$). The error bars are defined in the text.

physically grounded. Note that the calculation in the vacuum (using $\Delta_r G_g^*$) yields quite honorable results, in agreement with the discussion of section 3.3.

Anyway, the strong correlation of Figure 11 (top) shows that the number of ATZ molecules embedded in the polymer (related to Q_{FM} value) is the same as (or at least is proportional to) the total number of FM/ATZ and EDOT/ATZ dimers in the solution, before polymerization.

In Figure 11 (bottom), we have also considered the $Q_d \text{ FM-MICP}$ charges obtained from eq 2 and electrochemically measured. We have seen, in section 2, that these charges are related to the efficiency of the functionalized FM-MICP polymers to detect ATZ targets. It can be seen once again that the correlation with the total concentration of ATZ heterodimers ($[FM/ATZ] + [EDOT/ATZ]$) is strong ($R = 0.980$) but weaker than that for the Q_{FM} charge. This strong correlation can be found surprising, because several effects could disturb it:

- (1) The strength of the FM-ATZ interactions should interfere twice: first, in determining the number of FM/ATZ prepolymerization dimers and thus the number of functionalized cavities into the imprinted polymer during the polymerization process; second, in determining the efficiency of a given cavity to detect ATZ in the detection process.
- (2) The dimerization free energies in the functionalized cavities of the polymer are certainly different from those in the acetonitrile solution, and consequently, the FM/ATZ concentrations should have different values in the genuine polymer and in the FM-MICP matrix after detection.

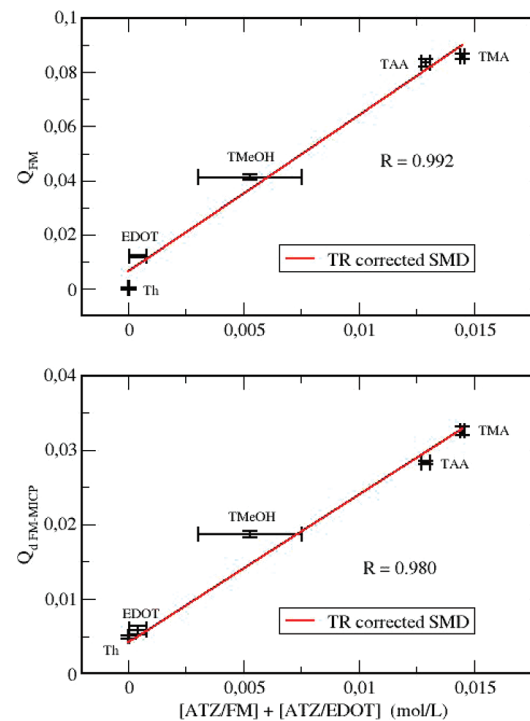


Figure 11. Correlation of the two experimental charges, Q_{FM} (top) and $Q_d \text{ FM-MICP}$ (bottom), with the total concentration of ATZ heterodimers, obtained using the most sophisticated calculation of the dimerization free energies ($\Delta_r G_{sol}^{TR \text{ mod } smd}$). The error bars are defined in the text.

- (3) ATZ molecules diffuse in the polymer at an unknown rate, depending on the nature of the FM-MICP polymer.

The fact that the correlation of Figure 11 (bottom) is strong suggests the following mechanism of atrazine detection:

- (1) The ATZ molecules diffuse slowly in the polymer matrix and independently of the nature of the FM-MICP, so that they are mainly collected by the imprinted cavities close to the polymer surface.
- (2) The imprinted cavities may thus be considered saturated by ATZ molecules in the detection process, so that the number of cavities does not interfere in this process.
- (3) The FM/ATZ dimerization free energies in the polymer matrixes are close to (or at least are proportional to) the free energies in the acetonitrile solution.

This good correlation shows that the detection of ATZ by FM-MICP polymer is simply related to the strength of the interaction between the ATZ target molecules and the FM functional monomers in the genuine solution. In particular, the number of FM/ATZ dimers in solution is the critical parameter which determines the efficiency of the FM-MICP toward the detection of ATZ.

5. CONCLUSION

In the present work, we experimentally and theoretically studied the influence of the nature of the chemical functionalities of a polythiophene-based molecularly imprinted conducting polymer (FM-MICP) on its ability to detect atrazine (ATZ) target molecule. A list of five functionalized thiophene-based monomers (FM = TMA, TAA, TMeOH, EDOT, and Th) was used in order to form FM/ATZ prepolymerization complexes in acetonitrile. After electrosynthesis, these complexes led to

FM-MICP sensitive layers deposited onto gold substrates and dedicated to the sensing of additional amounts of atrazine. We demonstrated, thanks to electrochemical measurements, the clear effect of the nature of FM functional monomer on the number of ATZ molecular imprints (Q_{FM} values) and on the sensitivity toward ATZ ($Q_{\text{d FM-MICP}}$ values) of the FM-MICP layers, which both decrease in the following order of FM functional monomers: TMA, TAA, TMeOH, EDOT, and Th. These experimental results were attributed to the strength of the FM-ATZ interaction.

For investigating this hypothesis, we performed DFT/SMD calculations of the free energies of formation of the FM/ATZ dimers in solution and deduced from these free energies the concentrations of the different FM/ATZ prepolymerization complexes present in acetonitrile medium before each FM-MICP electrosynthesis. The crude SMD values are poor, due to the poor treatment of entropy in the PCM formalism, but this entropy can be empirically introduced with the help of the Wertz formula. We have found a strong correlation between the measured electrochemical signals (Q_{FM} and $Q_{\text{d FM-MICP}}$ values) and the concentrations of the prepolymerization complexes, provided the empirical correction only uses the translation–rotation part of the entropy of the solutes and ignores the vibration part.

The good correlations demonstrate that a much elaborated property of the FM-MICP imprinted polymer, as is the detection of targets after a complex process of polymer synthesis and washing, can be very simply related to the strength of the interaction between the target molecules and the FM functional monomers in the genuine solution.

AUTHOR INFORMATION

Corresponding Author

*E-mail: pierre.archirel@u-psud.fr and samy.remita@u-psud.fr.

ACKNOWLEDGMENTS

We thank Pierre-Arnaud Artola, Fabien Caillez, and Pascal Pernot, from Laboratoire de Chimie Physique, for helpful discussions. All the calculations have been done on the computing cluster of the Laboratoire de Chimie Physique. We thank Jean-Marie Teuler for technical assistance.

REFERENCES

- (1) Mosbach, K.; Ramström, O. *Biotechnology* **1996**, *14*, 163–170.
- (2) Haupt, K.; Mosbach, K. *Chem. Rev.* **2000**, *100*, 2495–2504.
- (3) Shea, K. J. *Trends Polym. Sci.* **1994**, *2*, 166–173.
- (4) Wulff, G. *Angew. Chem., Int. Ed. Engl.* **1995**, *34*, 1812–1832.
- (5) Fu, Q.; Sanbe, H.; Kagawa, C.; Kunimoto, K.; Haginaka. *Anal. Chem.* **2003**, *75*, 191–198.
- (6) Li, P.; Rong, F.; Xie, Y.; Hu, V.; Yuan, C. *J. Anal. Chem.* **2004**, *59*, 939–944.
- (7) Holdsworth, C. I.; Bowyer, M. C.; Lennard, C.; McCluskey, A. *Aust. J. Chem.* **2005**, *58*, 315–320.
- (8) Ogawa, T.; Hoshina, K.; Haginaka, J.; Honda, C.; Tanimoto, T.; Uchida, T. *J. Pharm. Sci.* **2005**, *94*, 353–362.
- (9) Choong, C. L.; Milne, W. I. *Biosens. Bioelectron.* **2010**, *25*, 2384–2388.
- (10) Özcan, L.; Sahin, Y. *Sens. Actuators, B* **2007**, *127*, 362–369.
- (11) Pietrzyk, A.; Suriyanarayanan, S.; Kutner, W.; Chitta, R.; D’Souza, F. *Anal. Chem.* **2009**, *81*, 2633–2643.
- (12) Pardieu, E.; Cheap, H.; Vedrine, C.; Lazerges, M.; Lattach, Y.; Garnier, F.; Remita, S.; Pernelle, C. *Anal. Chim. Acta* **2009**, *649*, 236–245.
- (13) Lattach, Y.; Fourati, N.; Zerrouki, C.; Fougnion, J. M.; Garnier, F.; Remita, S. *Sens. Lett.* **2011**, *9*, 1–4.
- (14) Lattach, Y.; Garnier, F.; Remita, S. *ChemPhysChem.* **2012**, *13*, 281–290.
- (15) Meites, L. *Handbook of analytical chemistry*; McGraw-Hill: New York, 1963.
- (16) Shoji, R.; Takeuchi, T.; Kubo, I. *Anal. Chem.* **2003**, *75*, 4882–4886.
- (17) Garnier, F.; Korri Youssoufi, H.; Srivastava, P.; Yassar, A. *J. Am. Chem. Soc.* **1994**, *116*, 8813–8814.
- (18) Garnier, F.; Bouabdallaoui, B.; Srivastava, P.; Mandrand, B.; Chaix, C. *Sens. Actuators, B* **2007**, *123*, 13–20.
- (19) Tirapattur, S.; Belletête, M.; Drolet, N.; Leclerc, M.; Durocher, G. *Chem. Phys. Lett.* **2003**, *370*, 799–804.
- (20) Béra-Abérem, M.; Ho, H. A.; Leclerc, M. *Tetrahedron* **2004**, *60*, 11169–11173.
- (21) Doré, K.; Dubus, S.; Ho, H. A.; Lévesque, I.; Brunette, M.; Corbeil, G.; Boissinot, M.; Boivin, G.; Bergeron, M. G.; Boudreau, D.; Leclerc, M. *J. Am. Chem. Soc.* **2004**, *126*, 4240–4244.
- (22) Ho, H. A.; Leclerc, M. *J. Am. Chem. Soc.* **2004**, *126*, 1384–1387.
- (23) Tomasi, J.; Menucci, B.; Cammi, R. *Chem. Rev.* **2005**, *105*, 2999.
- (24) Marenich, A. V.; Cramer, C. J.; Truhlar, D. J. *J. Phys. Chem. B* **2009**, *113*, 6378–6396.
- (25) Frisch, M. J.; Trucks, G. W.; Schlegel, H. B.; Scuseria, G. E.; Robb, M. A.; Cheeseman, J. R.; Scalmani, G.; Barone, V.; Mennucci, B.; Petersson, G. A.; et al. *Gaussian 09*, revision A.02; Gaussian, Inc.: Wallingford, CT, 2009.
- (26) Cramer, Ch. *J. Essentials of Computational Chemistry*; Wiley: 2004; p 379.
- (27) Wong, P. M.; Piacenza, M.; Della Salla, F. *Phys. Chem. Chem. Phys.* **2009**, *11*, 4498–4508.
- (28) Grimme, S. *J. Comput. Chem.* **2006**, *27*, 1787–1799.
- (29) Fuentealba, P.; Preuss, H.; Stoll, H.; Szentpaly, L. *Chem. Phys. Lett.* **1989**, *89*, 418.
- (30) Hill, J. G.; Platts, J. A.; Werner, H. *J. Phys. Chem. Chem. Phys.* **2006**, *8*, 4072–4078.
- (31) Curtiss, L. A.; Frurip, D. J.; Blander, M. *J. Chem. Phys.* **1979**, *71*, 2703–2711.
- (32) McQuarrie, D. A. *Statistical Mechanics*; University Science Books: 2000.
- (33) Mammen, M.; Shaknovich, E. I.; Deutsch, J. M.; Whitesides, G. M. *J. Org. Chem.* **1998**, *63*, 3821–3830.
- (34) Siebert, X.; Amzel, M. *Proteins* **2004**, *54*, 104.
- (35) Swanson, J. M. J.; Henchman, R.; McCammon, J. A. *Biophys. J.* **2004**, *86*, 67–74.
- (36) Wertz, D. H. *J. Am. Chem. Soc.* **1980**, *102*, 5316–5322.
- (37) Ben Naim, A.; Marcus, Y. *J. Chem. Phys.* **1984**, *81*, 2016.
- (38) Cooper, J.; Ziegler, T. *Inorg. Chem.* **2002**, *41*, 6614.
- (39) Lau, J. K. C.; Deubel, D. V. *J. Chem. Theory Comput.* **2006**, *2*, 103.
- (40) Kua, J.; Hanley, S. W.; De Haan, D. O. *J. Phys. Chem. A* **2008**, *112*, 66.
- (41) Krtzner, H. E.; De Haan, D. O.; Kua, J. *J. Phys. Chem. A* **2009**, *113*, 6994.
- (42) Kua, J.; Krtzner, H. E.; De Haan, D. O. *J. Phys. Chem. A* **2011**, *115*, 1667.
- (43) Ahlquist, M.; Nielsen, R. J.; Periana, R. A.; Goddard, W. A. III. *J. Am. Chem. Soc.* **2009**, *131*, 17110.
- (44) Crowder, G. A.; Cook, B. R. *J. Chem. Phys.* **1967**, *71*, 914–916.
- (45) *Handbook of Chemistry and Physics*; CRC Press: 1994.
- (46) Murray, C. W.; Verdonk, M. *J. Comput.-Aided Mol. Des.* **2002**, *16*, 741–753.
- (47) Winkelmann, J. G. M.; Voorwinde, O. K.; Ottens, M.; Beenackers, A. A. C. M.; Janssen, L. P. B. M. *Chem. Eng. Sci.* **2002**, *57*, 4067.